ISSN 1674-1056
http://cpb.iphy.ac.cn
http://iopscience.iop.org/cpb
中国物理 B
Chinese Physics
中国物理 Chinese Physics B

Optimizing effective phase modulation in coupled double quantum well Mach-Zehnder modulators

Guang-Hui Wang(王光辉), Jin-Ke Zhang(张金珂)
Citation: Chin. Phys. B . 2018, 27(2): 027801. **doi:** 10.1088/1674-1056/27/2/027801

Journal homepage: http://cpb.iphy.ac.cn; http://iopscience.iop.org/cpb

What follows is a list of articles you may be interested in

Direct observation of the carrier transport process in InGaN quantum wells with a pn-junction

Haiyan Wu(吴海燕), Ziguang Ma(马紫光), Yang Jiang(江洋), Lu Wang(王禄), Haojun Yang(杨浩军), Yangfeng Li(李阳锋), Peng Zuo(左朋), Haiqiang Jia(贾海强), Wenxin Wang(王文新), Junming Zhou(周钧铭), Wuming Liu(刘伍明), Hong Chen(陈弘)
Chin. Phys. B . 2016, 25(11): 117803. **doi:** 10.1088/1674-1056/25/11/117803

Effects of multiple interruptions with trimethylindium-treatment in the InGaN/GaN quantum well on green light emitting diodes

Liang Qiao(乔良), Zi-Guang Ma(马紫光), Hong Chen(陈弘), Hai-Yan Wu(吴海燕), Xue-Fang Chen(陈雪芳), Hao-Jun Yang(杨浩军), Bin Zhao(赵斌), Miao He(何苗), Shu-Wen Zheng(郑树文), Shu-Ti Li(李述体)
Chin. Phys. B . 2016, 25(10): 107803. **doi:** 10.1088/1674-1056/25/10/107803

Exciton-phonon interaction in $Al_{0.4}Ga_{0.6}N/Al_{0.53}Ga_{0.47}N$ multiple quantum wells

Ya-Li Liu(刘雅丽), Peng Jin(金鹏), Gui-Peng Liu(刘贵鹏), Wei-Ying Wang(王维颖), Zhi-Qiang Qi(齐志强), Chang-Qing Chen(陈长清), Zhan-Guo Wang(王占国)
Chin. Phys. B . 2016, 25(8): 087801. **doi:** 10.1088/1674-1056/25/8/087801

Variation of efficiency droop with quantum well thickness in InGaN/GaN green light-emitting diode

Liu Wei, Zhao De-Gang, Jiang De-Sheng, Chen Ping, Liu Zong-Shun, Zhu Jian-Jun, Li Xiang, Liang Feng, Liu Jian-Ping, Yang Hui
Chin. Phys. B . 2015, 24(12): 127801. **doi:** 10.1088/1674-1056/24/12/127801

Effects of interface roughness on photoluminescence full width at half maximum in GaN/AlGaN quantum wells

Wang Wei-Ying, Liu Gui-Peng, Jin Peng, Mao De-Feng, Li Wei, Wang Zhan-Guo, Tian Wu, Chen Chang-Qing
Chin. Phys. B . 2014, 23(11): 117803. **doi:** 10.1088/1674-1056/23/11/117803

Optimizing effective phase modulation in coupled double quantum well Mach–Zehnder modulators*

Guang-Hui Wang(王光辉)[1,2,†] and Jin-Ke Zhang(张金珂)[1,2]

[1] *Guangzhou Key Laboratory for Special Fiber Photonic Devices South China Normal University, Guangzhou* 510006, *China*
[2] *Guangdong Provincial Key Laboratory of Nanophotonic Functional Materials and Devices, South China Normal University, Guangzhou* 510006, *China*

(Received 13 July 2017; revised manuscript received 16 October 2017; published online 5 January 2018)

We report optimal phase modulation based on enhanced electro–optic effects in a Mach–Zehnder (MZ) modulator constructed by AlGaAs/GaAs coupled double quantum well (CDQW) waveguides with optical gain. The net change of refractive indexes between two arms of the CDQW MZ modulator is derived by both the electronic polarization method and the normal-surface method. The numerical results show that very large refractive index change over 10^{-1} can be obtained, making the phase modulation in the CDQW MZ modulator very highly efficient. It is desirable and important that a very small voltage-length product for π phase shift, $V_\pi \times L_0 = 0.0226$ V·mm, is obtained by optimizing bias electric field and CDQW structural parameters, which is about seven times smaller than that in single quantum-well MZ modulators. These properties open an avenue for CDQW nanostructures in device applications such as electro–optical switches and phase modulators.

Keywords: electro–optic effect, phase modulator, quantum well

PACS: 78.20.Jq, 73.21.Fg, 42.65.–k **DOI:** 10.1088/1674-1056/27/2/027801

1. Introduction

Along with the renovation and advancement of modern nanotechnology, nanometer quantum devices, such as quantum-well modulators and lasers based on nonlinear optical effects in semiconductor nanostructures, have attracted extensive interest.[1–5] One reason is that there is very large optical nonlinearity in semiconductor nanostructures due to quantum-size effects and quantum-confinement effects of carriers in low-dimensional quantum systems, which is a significant property for nonlinear optical application.[6–9] Their optical nonlinearity can be controlled by structural parameters or applied electromagnetic fields. Another reason is that the growth of single atomic layer of good quality has become possible due to recent advances in material growth techniques, making various semiconductor nanostructures emerge such as coupled quantum wells and stepped quantum wells.[10–12] Therefore, quantum nanostructures become important candidates for electro–optic modulators.

It is well known that electro–optic modulators, utilizing an applied static electric field to modify the refractive index of a dielectric based on the electro–optic (Pockels or dc Kerr) effects, can be employed for phase and amplitude modulation of optical waves, etc.[13] To achieve a required depth of modulation for an electro–optic modulator with very low switching voltage and the smallest possible consumption of modulation power, many efforts have been made to enhance the electro–optic effects and improve the electro–optic modulators by either optimizing the confinement potential or integrating a compressively strained QW amplifier to compensate optical absorption loss in the QW modulator.[14–17] Another possible way of mitigating optical loss is to use a dielectric with optical gain to compensate optical loss in composite structures, such as semiconductor quantum dots.[18–21] Recently, we presented an effective approach to phase modulation in a Mach–Zehnder (MZ) modulator system constructed by a gain single QW nanostructure.[22] In this paper, we further investigate efficient phase modulation for transverse magnetic (TM) waves in coupled double quantum well (CDQW) MZ modulators based on enhanced electro–optic effects in AlGaAs/GaAs gain CDQW waveguides, where optical gain can be realized by proper doping or current injection. The novelty and the difference between our present work and related published papers are that: on the one hand, the CDQWs are chosen as waveguide arms, which have more advantages than single quantum systems, such as more flexible controllability and greater nonlinear coefficients; on the other hand, the CDQWs are of gain characteristics, which can compensate the losses of the waveguide system.

The present paper is organized as follows. In Section 2, electron states in CDQW waveguides with and without an applied electric field are derived. In Section 3, a basic framework for local electro–optic effect (Pockels effect) in CDQW MZ modulators with an applied electric field is presented by both

*Project supported by the National Natural Science Foundation of China (Grant No. 11474106), the Natural Science Foundation of Guangdong Province, China (Grant No. 2016A030313439), and the Science and Technology Program of Guangzhou City, China (Grant No. 201707010403).

†Corresponding author. E-mail: wanggh@scnu.edu.cn

© 2018 Chinese Physical Society and IOP Publishing Ltd

the electronic polarization method and the normal-surface one. In Section 4, the numerical results and discussion are presented for effective phase modulation in the CDQW MZ modulator. The numerical results show that very large positive refractive-index changes between two arms of the CDQW MZ modulator from resonant intersubband transition can attain to the order of magnitude of 10^{-1} by optimizing bias electric field and CDQW structural parameters. In addition, a very small voltage-length product for π phase shift is obtained as $V_\pi \times L_0 = 0.0226$ V·mm, which is about seven times smaller than that in single quantum-well MZ modulators. These novel properties may have potential application in high-performance and high-miniaturization nano quantum devices. Brief conclusions are given in Section 5.

2. Electron states in CDQW waveguides

To start, we design an MZ phase modulator constructed by CDQW waveguides, as shown in Fig. 1. Each arm of the MZ phase modulator is replaced by the same AlGaAs/GaAs CDQW waveguides confined in the z direction. The bias electric field E_d is applied on one arm (arm II) of the MZ modulator along the z direction, as shown in Fig. 1(b). The waveguides are along the x direction, and the E field in the waveguides is z-directed. L_0 is the propagation length of the light wave inside the CDQW waveguides. Based on the effective mass approximation, the Schrödinger equation for an electron in CDQWs with an applied electric field can be written as

$$\left[-\frac{\hbar^2}{2m^*}\nabla^2 + V(z) - ezE_\mathrm{d}\right]\psi_{n,q}(\boldsymbol{r}) = E_{n,q}\psi_{n,q}(\boldsymbol{r}), \qquad (1)$$

with the confinement potential $V(z)$

$$V(z) = \begin{cases} V_2, & z < -z_3, \\ 0, & -z_3 < z < -z_1, \\ V_1, & -z_1 < z < z_1, \\ 0, & z_1 < z < z_2, \\ V_2, & z > z_2, \end{cases} \qquad (2)$$

where z represents the confinement direction of the CDQWs; V_1 and V_2 denote the mid-barrier and outer barrier height, respectively; $\hbar$ is Planck constant; e is electron charge; E_d is the applied electric field; m^* is the effective mass of an electron in the conduction band; $\psi_{n,q}(\boldsymbol{r})$ and $E_{n,q}$ denote the eigenfunctions and eigenenergies of the CDQW nanostructures, respectively. Due to the system with the translational invariance in xy plane and the confinement in the z direction, $\psi_{n,q}(\boldsymbol{r})$ and $E_{n,q}$ can be written as

$$\psi_{n,q}(\boldsymbol{r}) = \frac{1}{2\pi}\mathrm{e}^{\mathrm{i}\boldsymbol{q}_\parallel\cdot\boldsymbol{r}_\parallel}\varphi_n(z), \qquad (3)$$

and

$$E_{n,q} = \varepsilon_n + \frac{\hbar^2}{2m^*}|\boldsymbol{q}_\parallel|^2, \qquad (4)$$

here, $\boldsymbol{q}_\parallel$ and $\boldsymbol{r}_\parallel$ are electron wave vector and position vector in the xy plane. $\varphi_n(z)$ and ε_n, solutions of one-dimensional Schrödinger equation $H_0\varphi_n(z) = \varepsilon_n\varphi_n(z)$ with $H_0 = -(\hbar^2/2m^*)(\mathrm{d}^2/\mathrm{d}z^2) + V(z) - ezE_\mathrm{d}$, are called the envelope wavefunctions and corresponding energy eigenvalue of the nth subband, respectively.

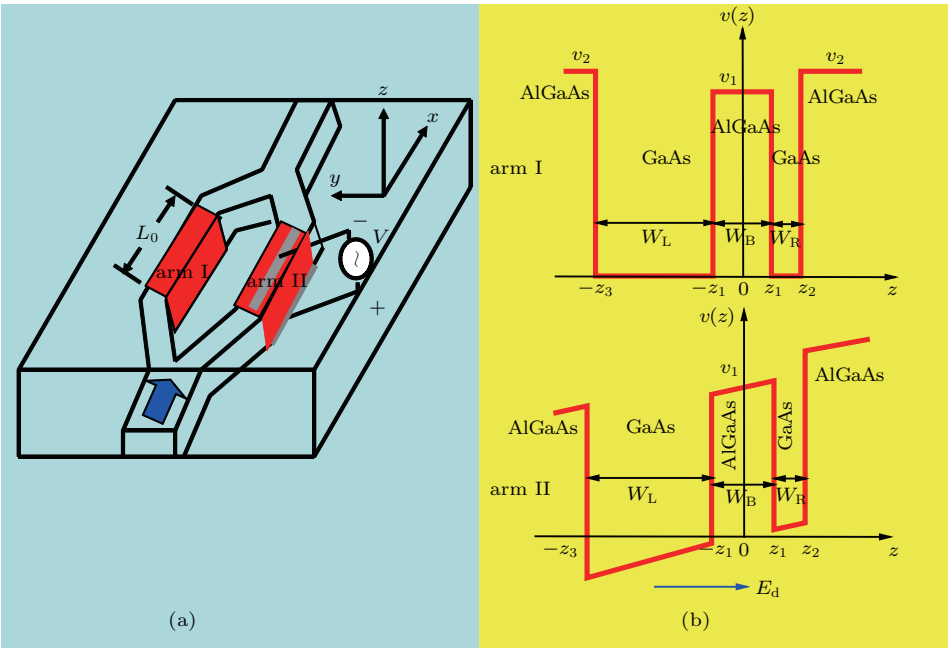


Fig. 1. (color online) (a) The schematic diagram of the CDQW MZ modulator. Two red regions denote two arms (arm I and arm II) constructed by the CDQW waveguides. Two grey strips denote electrodes, located at the top and bottom of the arm II with an applied bias voltage V, respectively. The blue arrow denotes incident field with electric-field polarization along the z direction. (b) The AlGaAs/GaAs CDQW configuration without (arm I) and with (arm II) an applied electric field, and confinement direction, where W_L, W_R, and W_B denote the left-well, right-well, and mid-barrier width, respectively.

For the finite-depth CDQW, $\varphi_n(z)$ and ε_n of the CDQW in the presence of an applied electric field can be expressed as[8,23]

$$\varphi_n(z)=\begin{cases} a_n\exp(\xi_1 z), & z<-z_3;\\ b_{1n}\mathrm{Ai}(\xi_2 z)+b_{2n}\mathrm{Bi}(\xi_2 z), & -z_3<z<-z_1,\\ c_{1n}\mathrm{Ai}(\xi_3 z)+c_{2n}\mathrm{Bi}(\xi_3 z), & -z_1<z<z_1,\\ d_{1n}\mathrm{Ai}(\xi_2 z)+d_{2n}\mathrm{Bi}(\xi_2 z), & z_1<z<z_2,\\ e_n\exp(-\xi_4 z), & z>z_2, \end{cases} \quad (5)$$

where Ai and Bi are Airy functions; $\xi_1=[2m^*(V_2-\varepsilon_n+ezE_\mathrm{d})]^{1/2}/\hbar$, $\xi_2=[(2m^*eE_\mathrm{d})/\hbar^2]^{1/3}[z-\varepsilon_n/(eE_\mathrm{d})]$, $\xi_3=[(2m^*eE_\mathrm{d})/\hbar^2]^{1/3}[z+(V_1-\varepsilon_n)/(eE_\mathrm{d})]$, $\xi_4=[2m^*(V_2-\varepsilon_n+ezE_\mathrm{d})]^{1/2}/\hbar$. The coefficients ($a_n$, b_{1n}, b_{2n}, c_{1n}, c_{2n}, d_{1n}, d_{2n}, e_n) and the energy eigenvalue ε_n can be obtained numerically through the continuity of envelope wavefunctions and their first derivative at the boundaries.

In the absence of an applied electric field, however, $\varphi_n(z)$ and ε_n in the CDQW can be expressed as[8,23]

$$\varphi_n(z)=\begin{cases} a'_n\exp(k_1 z), & z<-z_3,\\ b'_{1n}\sin(k_2 z)+b'_{2n}\cos(k_2 z), & -z_3<z<-z_1,\\ c'_{1n}\exp(k_3 z)+c'_{2n}\exp(-k_3 z), & -z_1<z<z_1,\\ d'_{1n}\sin(k_2 z)+d'_{2n}\cos(k_2 z), & z_1<z<z_2,\\ e'_n\exp(-k_1 z), & z>z_2, \end{cases} \quad (6)$$

where $k_1=\sqrt{2m^*(V_2-\varepsilon_n)}/\hbar$, $k_2=\sqrt{2m^*\varepsilon_n}/\hbar$, and $k_3=\sqrt{2m^*(V_1-\varepsilon_n)}/\hbar$. The coefficients ($a'_n$, b'_{1n}, b'_{2n}, c'_{1n}, c'_{2n}, d'_{1n}, d'_{2n}, e'_n) and the energy eigenvalue ε_n can also be obtained numerically through the continuity of envelope wavefunctions and their first derivative at the boundaries.

3. Electro–optic effect in CDQW MZ modulators

3.1. Electronic polarization method

Let us consider a linear-polarized dichromatic light with polarization along the z direction is incident on the CDQW waveguide. Due to the CDQW system with translation invariance along the xy direction, the time-harmonic electric field $\boldsymbol{E}(\boldsymbol{r},t)$ and polarization $\boldsymbol{P}(\boldsymbol{r},t)$ have the following form

$$\boldsymbol{E}(\boldsymbol{r},t)=\sum_{l=1,2}[\widetilde{\boldsymbol{E}}(z;\omega_l)\,\mathrm{e}^{\mathrm{i}(\boldsymbol{k}_{||l}\cdot\boldsymbol{r}_{||}-\omega_l t)}+\mathrm{c.c.}], \quad (7)$$

$$\boldsymbol{P}(\boldsymbol{r},t)=\sum_{l=1,2}[\widetilde{\boldsymbol{P}}(z;\omega_l)\,\mathrm{e}^{\mathrm{i}(\boldsymbol{k}_{||l}\cdot\boldsymbol{r}_{||}-\omega_l t)}+\mathrm{c.c.}], \quad (8)$$

where $\boldsymbol{k}_{||}=(k_x,k_y,0)$ stands for the wave vector in the xy plane of the incident light. By inserting Eqs. (7) and (8) into Maxwell's equations, we can derive the differential equation for the electric field $\widetilde{\boldsymbol{E}}(z;\omega)$, viz,

$$\begin{aligned}&\overleftrightarrow{\Lambda}(\omega)\cdot\widetilde{\boldsymbol{E}}(z;\omega)\\ &=-\frac{\omega^2}{c^2}[\varepsilon_\mathrm{B}(\omega)\widetilde{\boldsymbol{E}}(z;\omega)+\widetilde{\boldsymbol{P}}^{(1)}(z;\omega)+\widetilde{\boldsymbol{P}}^{(2)}(z;\omega)], \end{aligned}\quad (9)$$

with

$$\widetilde{\boldsymbol{P}}^{(1)}(z;\omega)=\overleftrightarrow{\chi}^{(1)}(\omega)\cdot\widetilde{\boldsymbol{E}}(z;\omega), \quad (10)$$

and

$$\widetilde{\boldsymbol{P}}^{(2)}(z;\omega)=\sum_{\omega_1+\omega_2=\omega}\overleftrightarrow{\chi}^{(2)}(\omega_1,\omega_2):\widetilde{\boldsymbol{E}}(z;\omega_1)\widetilde{\boldsymbol{E}}(z;\omega_2), \quad (11)$$

where $\overleftrightarrow{\chi}^{(1)}$ and $\overleftrightarrow{\chi}^{(2)}$ stand for the local linear and second-order nonlinear susceptibility tensors for the CDQW system, respectively. The tensorial operator $\overleftrightarrow{\Lambda}(\omega)=\overleftrightarrow{I}[-k_{||}^2+\partial^2/\partial z^2]$, where $\overleftrightarrow{I}$ denotes the unit tensor. $\varepsilon_\mathrm{B}(\omega)=1+\chi_\mathrm{b}(\omega)$ is the relative dielectric constant for the isotropic background medium and the contribution from the nonresonant polarization described by the background susceptibility $\chi_\mathrm{b}(\omega)$ of the conduction-band electrons in the CDQW.

By substituting Eqs. (10) and (11) into (9), and assuming $\widetilde{\boldsymbol{E}}(z;\omega_1)$ is dc field denoted by $\boldsymbol{E}_\mathrm{d}$ in the following, one can obtain the following equation for the electric field $\widetilde{\boldsymbol{E}}(z;\omega)$

$$\overleftrightarrow{\Lambda}(\omega)\cdot\widetilde{\boldsymbol{E}}(z;\omega)+\frac{\omega^2}{c^2}\overleftrightarrow{\varepsilon}_\mathrm{d}(\omega,E_\mathrm{d})\cdot\widetilde{\boldsymbol{E}}(z;\omega)=0, \quad (12)$$

with

$$\begin{aligned}\overleftrightarrow{\varepsilon}(\omega,E_\mathrm{d}) &= \varepsilon^B(\omega)\overleftrightarrow{I}+\overleftrightarrow{\chi}^{(1)}(\omega,E_\mathrm{d})\\ &\quad+2\overleftrightarrow{\chi}^{(2)}(\omega,E_\mathrm{d})\cdot\boldsymbol{E}_\mathrm{d}. \end{aligned}\quad (13)$$

As both the polarization of the incident electric field and the confinement direction of the CDQW waveguide are directed along the z direction, we only need to consider the ε_{zz} component of the dielectric function tensor, namely,

$$\varepsilon_{zz}(\omega,E_\mathrm{d})=\varepsilon^B(\omega)+\chi^{(1)}_{zz}(\omega,E_\mathrm{d})+2\chi^{(2)}_{zzz}(\omega,E_\mathrm{d})E_\mathrm{d}, \quad (14)$$

where $\chi^{(1)}_{zz}$ and $\chi^{(2)}_{zzz}$ stand for the local linear and second-order nonlinear susceptibility in the confinement direction of the CDQW waveguide, respectively, which can be obtained as[18–20]

$$\chi^{(1)}_{zz}(\omega,E_\mathrm{d}) = \frac{Ne^2[f_\mathrm{c}(\varepsilon_1)-f_\mathrm{c}(\varepsilon_2)]|M_{21}|^2}{\varepsilon_0(\varepsilon_{21}-\hbar\omega-\mathrm{i}\hbar\Gamma_{12})}, \quad (15)$$

$$\begin{aligned}\chi^{(2)}_{zzz}(\omega,E_\mathrm{d}) &= \frac{Ne^3|M_{21}|^2(M_{22}-M_{11})[f_\mathrm{c}(\varepsilon_1)-f_\mathrm{c}(\varepsilon_2)]}{\varepsilon_0}\\ &\quad\times\left[\frac{1}{(\varepsilon_{21}-\hbar\omega-\mathrm{i}\hbar\Gamma_{12})(\hbar\omega+\mathrm{i}\hbar\Gamma_{11})}\right.\\ &\quad\left.+\frac{1}{(\varepsilon_{21}-\hbar\omega-\mathrm{i}\hbar\Gamma_{12})^2}\right], \end{aligned}\quad (16)$$

where $M_{nm}=\int_{-\infty}^{+\infty}\varphi_n^* z\varphi_m\,\mathrm{d}z$ and $\varepsilon_{21}=\varepsilon_2-\varepsilon_1$, here $\varphi_n(z)$ and ε_n ($n=1,2$) are the envelope wavefunctions and corresponding energy eigenvalues of the n-th subband of the two-level CDQW, respectively. ε_0 is the vacuum permittivity. Γ_{11} and Γ_{12} are the diagonal and nondiagonal non-radiative relaxation rate, respectively. $f_\mathrm{c}(\varepsilon_n)$ is the carrier distribution function in the n-th subband. N is the dipole density.

3.2. Normal-surface method

It is well known that the CDQW system behaves as a uniaxial optical medium in the absence of an applied electric field, due to different optical properties in the confinement and unconfinement directions. According to the configuration of the CDQW waveguides, as mentioned in Fig. 1(b), the optical axis is along the z direction, the equation for the index ellipsoid can be expressed as

$$\frac{x^2}{n_0^2}+\frac{y^2}{n_0^2}+\frac{z^2}{n_z^2}=1, \tag{17}$$

where n_0 and n_z are the linear refractive indexes in the no confinement and confinement directions in the CDQW waveguides, respectively. The nonzero elements of the electro–optic tensor of the CDQW system are $\gamma_{41}=\gamma_{52}=\gamma_{63}$ and γ_{33},[13] its matrix form can be written as

$$\begin{bmatrix} 0 & 0 & 0 \\ 0 & 0 & 0 \\ 0 & 0 & \gamma_{33} \\ \gamma_{41} & 0 & 0 \\ 0 & \gamma_{52} & 0 \\ 0 & 0 & \gamma_{63} \end{bmatrix}.$$

In the presence of an applied electric field E_d, however, the index ellipsoid of the CDQW system is expressed as

$$\frac{1}{n_0^2}x^2+\frac{1}{n_0^2}y^2+\left(\frac{1}{n_z^2}+\gamma_{33}E_\mathrm{d}\right)z^2+2\gamma_{41}E_\mathrm{d}xy=1, \tag{18}$$

by the coordinate transformation, the equation of the index ellipsoid in the coordinate system aligned with the new principle axis can be obtained as

$$\left(\frac{1}{n'_{xx}}\right)^2x^2+\left(\frac{1}{n'_{yy}}\right)^2y^2+\left(\frac{1}{n'_{zz}}\right)^2z^2=1, \tag{19}$$

with

$$n'_{xx}\simeq n_0+\frac{1}{2}n_0^3\gamma_{41}E_\mathrm{d}, \tag{20a}$$

$$n'_{yy}\simeq n_0-\frac{1}{2}n_0^3\gamma_{41}E_\mathrm{d}, \tag{20b}$$

$$n'_{zz}\simeq n_z-\frac{1}{2}n_z^3\gamma_{33}E_\mathrm{d}, \tag{20c}$$

where n_z and γ_{33} are: $n_z=\{\varepsilon_\mathrm{B}+\mathrm{Re}[\chi^{(1)}_{zz}(\omega,E_\mathrm{d})]\}^{1/2}$ and $\gamma_{33}=-2\chi^{(2)}_{zzz}(\omega,E_\mathrm{d})/n_z^4$.[13,22]

4. Numerical results and discussion

In what follows we will discuss the local electro–optic effect and effective phase modulation in the MZ modulator constructed by AlGaAs/GaAs CDQW waveguides from resonant intersubband transition of electrons in conduction bands. Based on Eqs. (14) and (20c), the optical gain coefficient can be written as[18,22]

$$g(\omega,E_\mathrm{d})=-\omega/(cn_0)\,\mathrm{Im}[\chi^{(1)}_{zz}(\omega)+2\chi^{(2)}_{zzz}(\omega)E_\mathrm{d}], \tag{21}$$

and the net change of refractive indexes between two arms in the confinement direction is

$$\begin{aligned}\Delta n &= n'_{zz}(\omega,E_\mathrm{d})-n_z(\omega,0)\\ &= \sqrt{\varepsilon_{zz}(\omega,E_\mathrm{d})}-\sqrt{\varepsilon_{zz}(\omega,0)},\end{aligned} \tag{22}$$

where $n'_{zz}(\omega,E_\mathrm{d})$ denotes the refractive index of the arm with nonlinear response in the presence of an applied electric field E_d, and $n_z(\omega,0)$ denotes the refractive index of the other arm with the linear response in the absence of an applied electric field E_d. Then the phase difference of two arms is $\Delta\phi=\omega\Delta nL_0V/(cE_\mathrm{d}W)$,[13] where c is the velocity of light in vacuum, W is the total height of the CDQW waveguides in the z direction, and V is the bias voltage corresponding to the applied electric field E_d. The voltage-length product for π phase shift can be obtained as[22]

$$V_\pi\times L_0=\frac{\lambda E_\mathrm{d}W}{2\Delta n}, \tag{23}$$

where V_π denotes the required voltage for π phase shift, and λ is the wavelength of incident light. Some parameters for AlGaAs/GaAs CDQW waveguides used in the following calculation are adopted as: $m^*=0.067m_0$ (m_0 is the mass of a free electron), $\varepsilon_\mathrm{B}=13.1$, $N=10^{17}/\mathrm{cm}^3$, $n_0=3.62$, and $\hbar\Gamma_{11}=\hbar\Gamma_{12}=4.7$ meV.[6,22–25] Due to the population inversion which can be achieved by laser pumping or ion injection, $f_\mathrm{c}(\varepsilon_1)=0$, and $f_\mathrm{c}(\varepsilon_2)=1$.[18,19] The total CDQW structure is designed such as applied bias drops across only 0.285 μm,[14] namely $W=0.285$ μm.

The modulation characteristics of the optical gain spectra in Fig. 2(a) and the net refractive-index change Δn between two arms in Fig. 2(b) are shown as a function of the wavelength of incident light λ under various applied electric fields E_d, with $W_\mathrm{L}=W_\mathrm{R}=0.5$ nm, $W_\mathrm{B}=0.25$ nm, and $V_1=V_2=5$ eV. From Fig. 2(a), we can see that optical gain occurs due to the population inversion, and the optical gain coefficient is very large at resonance. In addition, the gain spectrum is wide. These properties are very desirable and important in the design of an electro–optic modulator for compensating the consumption of modulation power. From the spectra of the net refractive-index change in Fig. 2(b), we can see that there exists a positive maximum, $(\Delta n)_\mathrm{max}$, in the vicinity of the resonance, which is over the order of magnitude of 10^{-3} in the presence of a suitable bias electric field. In addition, the net change of refractive index is closely dependent on the applied electric field. With the increase of the applied electric field, Δn becomes larger and larger.

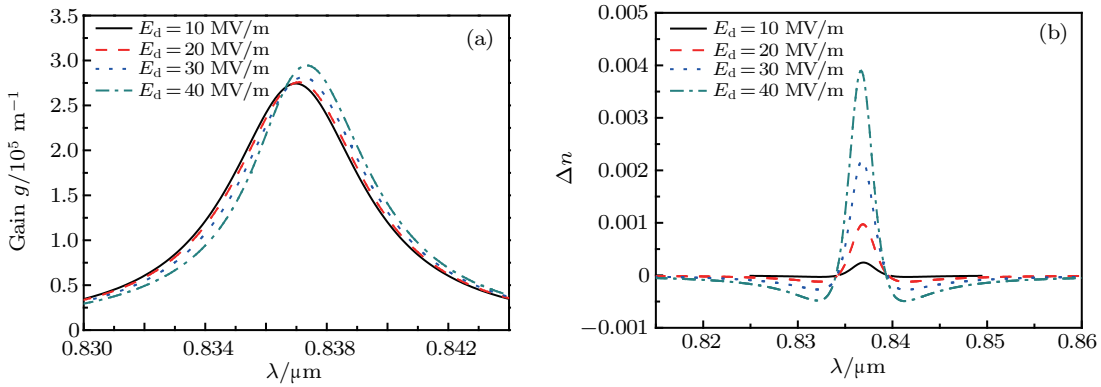


Fig. 2. (color online) The optical gain coefficient, g, in (a) and the net change of refractive indexes between two arms, Δn, in (b) as a function of the wavelength of incident light, λ, under various applied electric fields, respectively.

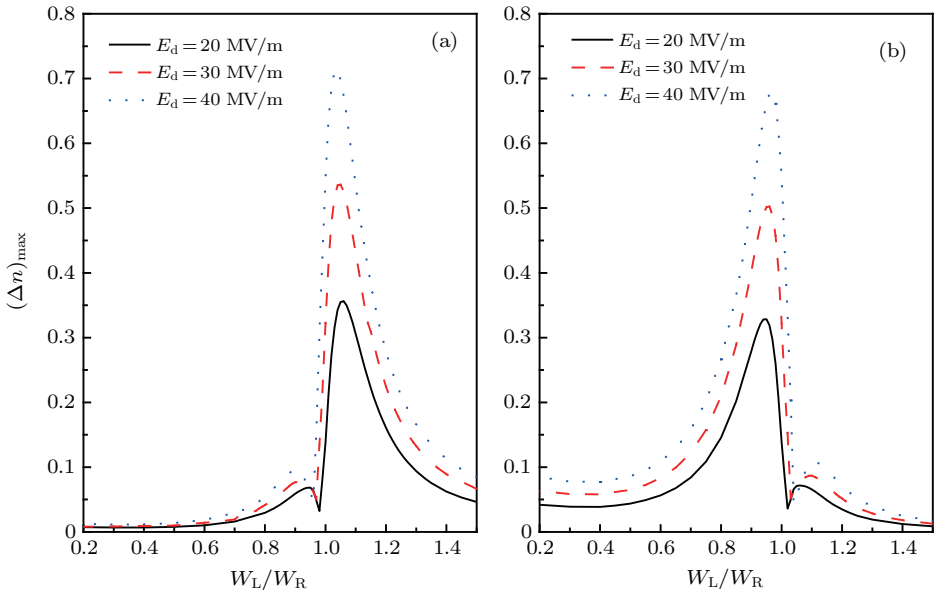


Fig. 3. (color online) The maximum net change of refractive index $(\Delta n)_{max}$ versus the well-width ratio W_L/W_R with $W_R = 1$ nm in (a), and the well-width ratio W_R/W_L with $W_L = 1$ nm in (b), under various applied electric fields.

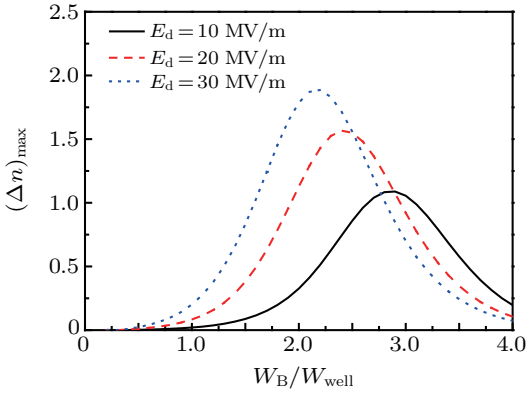


Fig. 4. (color online) The maximum net change of refractive index $(\Delta n)_{max}$ versus the normalized mid-barrier width W_B/W_{well} for three different applied electric fields E_d, with $W_{well} = 1$ nm.

To see the change of $(\Delta n)_{max}$ with the variation of the width of the left-side well, right-side well and mid-barrier, we plot $(\Delta n)_{max}$ versus the well-width ratio W_L/W_R with $W_R = 1$ nm in Fig. 3(a), and the well-width ratio W_R/W_L with $W_L = 1$ nm in Fig. 3(b), under the condition of a variety of applied electric fields. In addition, $W_B = 1$ nm and $V_1 = V_2 = 5$ eV. From Fig. 3, we can see that there is a peak for the variation of $(\Delta n)_{max}$, indicating that a suitable well-width ratio can be chosen to make $(\Delta n)_{max}$ maximum. It is worth noting that the peak position of $(\Delta n)_{max}$ holds basically at $W_L/W_R = 1.05$ or $W_R/W_L = 0.96$ for different applied electric fields, and the peak value can attain to the order of magnitude of 10^{-1}. The very large change of the refractive index would be of advantage to enhance phase modulation efficiency and performance in optoelectronic devices. In Fig. 4, $(\Delta n)_{max}$ is plotted as a function of the normalized mid-barrier width, W_B/W_{well}, for three different applied electric fields with $W_{well} = W_L = W_R = 1$ nm, and $V_1 = V_2 = 2$ eV, respectively. Similarly there is an optimal mid-barrier width in order to obtain a maximal change of refractive index for a fixed applied electric field. This is because the coupling effects between the left and right wells become the strongest under the condition of the optimal mid-barrier width. As the applied electric field increases, the optimal mid-barrier width will become narrower.

In Fig. 5, the maximum net refractive-index change

$(\Delta n)_{\max}$ (solid lines) and corresponding wavelength λ of incident light (dashed lines) are shown as a function of applied bias electric fields $E_{\rm d}$, where figures 5(a), 5(b), 5(c), and 5(d) correspond to $W_{\rm B}/W_{\rm well} = 1.0$, 2.2, 2.4, 2.9 with $W_{\rm well} = W_{\rm L} = W_{\rm R} = 1$ nm and $V_1 = V_2 = 2$ eV, respectively. From Fig. 5, we can see that the variation law of $(\Delta n)_{\max}$ with the applied electric field is closely dependent on the mid-barrier width $W_{\rm B}$. Concretely speaking, $(\Delta n)_{\max}$ increases monotonously with the applied electric field increasing when the mid-barrier width $W_{\rm B}$ is narrow (such as $W_{\rm B}/W_{\rm well} = 1.0$), but when $W_{\rm B}/W_{\rm well} \geq 2.2$, $(\Delta n)_{\max}$ first increases and then decreases with the applied electric field increasing. Their corresponding wavelength would always decrease gradually due to the increase of the energy-level interval of the CDQW induced by the applied electric field. This is because the wavelength is inversely proportional to the energy level interval of the CDQW. Very large refractive-index changes in the CDQW nanostructures are attributed mainly to two aspects: (i) satisfying transition resonance conditions; (ii) very large nonlinear coefficients in the CDQWs due to very strong coupling effects between the left and right wells, which can be optimized by tuning the CDQW structural parameters and bias voltage.

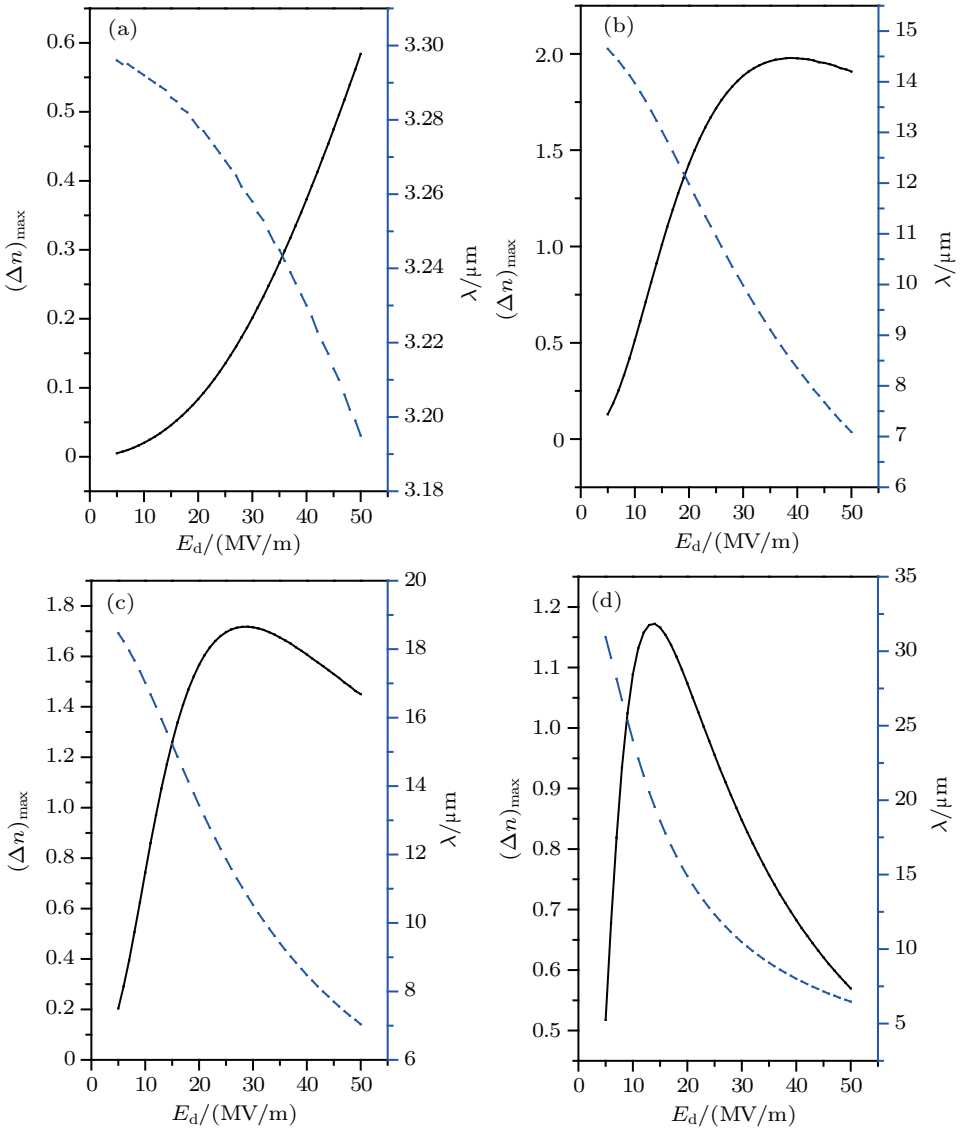


Fig. 5. (color online) The maximum net change of refractive index $(\Delta n)_{\max}$ (solid line) and corresponding wavelength λ (dashed line) versus the applied bias electric field $E_{\rm d}$. Panels (a), (b), (c), and (d) correspond to $W_{\rm B}/W_{\rm well} = 1.0$, 2.2, 2.4, 2.9 with $W_{\rm well} = 1$ nm, respectively.

In order to demonstrate further the phase modulation properties in the CDQW MZ modulator, the voltage-length product $(V_\pi \times L_0)$ for π phase shift is shown as a function of applied bias electric fields $(E_{\rm d})$ in Fig. 6, for four different normalized mid-barrier widths: $W_{\rm B}/W_{\rm well} = 1.0$ (black line), 2.2 (red line), 2.4 (blue line), 2.9 (dark cyan line) with $W_{\rm well} = W_{\rm L} = W_{\rm R} = 1$ nm and $V_1 = V_2 = 2$ eV, respectively. From Fig. 6, it is not hard to see that the voltage-length product tends to infinity when $E_{\rm d}$ tends to 0. This is because the net refractive-index change $\Delta n = 0$ when $E_{\rm d} = 0$. In addition, we can also see that when the mid-barrier width is narrow (such as $W_{\rm B}/W_{\rm well} = 1.0$), the voltage-length product decreases grad-

ually with the applied electric field increasing, while it has a minimum when $W_B/W_{well} \geq 2.2$. For $W_B/W_{well} = 2.2$, the minimum voltage–length product is 22.55×10^{-6} V·m when $E_d = 28$ MV/m. For $W_B/W_{well} = 2.4$, the minimum voltage–length product is 24.45×10^{-6} V·m when $E_d = 21$ MV/m. For $W_B/W_{well} = 2.9$, the minimum voltage–length product is 31.45×10^{-6} V·m when $E_d = 10$ MV/m. From these properties, we can find that the phase modulation efficiency can be optimized by choosing a suitable single-arm driving voltage and optimal structural parameters of the CDQWs. For instance, when $W_B/W_{well} = 2.2$ and $E_d = 28$ MV/m, the voltage–length product is $V_\pi \times L_0 = 22.55 \times 10^{-6}$ V · m, which is about seven times smaller than that in the phase modulator constructed by single quantum-well nanostructures,[22] meaning that the propagation length of TM waves for π phase shift is only $L_0 = 2.826$ μm under the single-arm driving voltage $V_0 = 7.98$ V. The very low bias voltage and small propagation length is very advantageous for the miniaturization and integration of quantum devices. The mechanism for this efficiency enhancement of the phase modulation is the resonant transition and very large dipole transition matrix elements, induced by optimizing bias electric field and CDQW structural parameters. These properties open an avenue for CDQW nanostructures in device applications such as electro–optical switches and phase modulators.

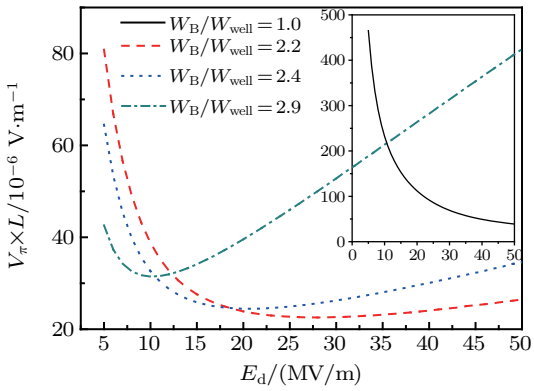


Fig. 6. (color online) The voltage-length product $V_\pi \times L_0$ for π phase shift versus the applied bias electric field E_d for four different normalized mid-barrier widths: $W_B/W_{well} = 1.0$ (black line), 2.2 (red line), 2.4 (blue line), 2.9 (dark cyan line) with $W_{well} = 1$ nm, respectively.

5. Conclusions

In this paper, the enhanced electro–optic effects and their effective phase-modulation application for TM waves in an MZ modulator constructed by gain CDQW waveguides have been demonstrated in detail. We have shown very large optical gain coefficient and wide gain spectrum, which are very desirable and important properties in the practical applications of electro–optic modulators for compensating the consumption of modulation power. We have demonstrated that it is possible that effective phase modulation in the CDQW MZ modulator is optimized by adopting a suitable bias voltage and CDQW structural parameters to reduce the size and modulation voltage of the device. We have obtained a very large change of refractive index, as well as a very small voltage–length product for π phase shift between two arms of the CDQW MZ modulator, which is about seven times smaller than that in single quantum-well MZ modulators. These properties indicate how unique CDQW electro–optic effect can be exploited in high-performance and high-miniaturization nano quantum devices.

References

[1] Moreau G, Martinez A, Cong D Y, Merghem K, Miard A, Lemaitre A, Voisin P, Ramdane A, Krestnikov I, Kovsh A R, Fischer M and Koeth J 2007 *Appl. Phys. Lett.* **91** 091118

[2] Jiang H T and Singh J 1999 *Appl. Phys. Lett.* **75** 1932

[3] Asadpour S H and Soleimani R H 2014 *Chin. Phys. B* **23** 104205

[4] Wei S H, Ma B, Chen Z S, Liao Y P, Hao H Y, Zhang Y, Ni H Q and Niu Z C 2017 *Chin. Phys. B* **26** 074208

[5] Salem E B, Chaabani R and Jaziri S 2016 *Chin. Phys. B* **25** 098101

[6] Wang G H 2005 *Phys. Rev. B* **72** 155329

[7] Xie W F 2014 *J. Lumin.* **145** 283

[8] Chen B, Guo K X, Liu Z L, Wang R Z, Zheng Y B and Li B 2008 *J. Phys.: Condens. Matter* **20** 255214

[9] Yildirim H and Tomak M 2005 *Phys. Rev. B* **72** 115340

[10] Zhu H Y, Zhang T Y and Zhao W 2009 *J. Appl. Phys.* **105** 043518

[11] Kouhi M, Vahedi A, Akbarzadeh A, Hanifehpour Y and Joo S W 2014 *Nanoscale Research Letters* **9** 131

[12] Gudiksen M S, Lauhon L J, Wang J, Smith D C and Lieber C M 2002 *Nature* **415** 617

[13] Haus H A 1984 *Waves and fields in optoelectronics* (New Jersey: Prentice-Hall)

[14] Zucker J E, Jones K L, Miller B I, Young M G, Koren U, Evankow J D and Burrus C A 1992 *Appl. Phys. Lett.* **60** 277

[15] Mohseni H, An H, Shellenbarger Z A, Kwakernaak M H and Abeles J H 2005 *Appl. Phys. Lett.* **86** 031103

[16] Xu Z X, Wang C R, Qi W and Yuan Z F 2010 *Opt. Lett.* **35** 736

[17] Mohseni H, An H, Shellenbarger Z A, Kwakernaak M H and Abeles J H 2004 *Appl. Phys. Lett.* **84** 1823

[18] Holmström P, Thylén L and Bratkovsky A 2010 *J. Appl. Phys.* **107** 064307

[19] Holmström P, Thylén L and Bratkovsky A 2010 *Appl. Phys. Lett.* **97** 073110

[20] Park S H, Ahn D and Kim J W 2008 *Appl. Phys. Lett.* **92** 171115

[21] Cooney R R, Sewall S L, Sagar D M and Kambhampati P 2009 *Phys. Rev. Lett.* **102** 127404

[22] Wang G H and Wang R Q 2015 *Opt. Commun.* **344** 161

[23] Wang C Y and Wang G H 2014 *Chin. Phys. B* **23** 127103

[24] Roan E J and Chuang S L 1991 *J. Appl. Phys.* **69** 3249

[25] Ahn D and Chuang S L 1987 *J. Appl. Phys.* **62** 3052